Distributed Platoon Control Under Topologies With Complex Eigenvalues: Stability Analysis and Controller Synthesis

Shengbo Eben Li[®], *Senior Member*, *IEEE*, Xiaohui Qin, Yang Zheng[®], Jianqiang Wang, Keqiang Li, and Hongwei Zhang, *Senior Member*, *IEEE*

Abstract—The platooning of autonomous vehicles can significantly benefit road traffic. Most previous studies on platoon control have only focused on specific communication topologies, especially those with real eigenvalues. This paper extends existing studies on distributed platoon control to more generic topologies with complex eigenvalues, including both internal stability analysis and linear controller synthesis. Linear platoon dynamics are derived using an inverse vehicle model compensation, and graph theory is employed to model the communication topology, leading to an integrated high-dimension linear model of the closedloop platoon dynamics. Using the similarity transformation, a sufficient and necessary condition is derived for the internal stability, which is completely defined in real number field. Then, we propose a Riccati inequality based algorithm to calculate the feasible static control gain. Further, disturbance propagation is formulated as an H_{∞} performance, and the upper bound of spacing errors is explicitly derived using Lyapunov analysis. Numerical simulations with a nonlinear vehicle model validate the effectiveness of the proposed methods.

Index Terms—Autonomous vehicle, disturbance propagation, internal stability, platoon.

I. INTRODUCTION

UTONOMOUS driving is the current trend of intelligent transportation systems. To meet the social demand on improving safety and efficiency, emerging technologies such as lidar, differential global position system, and high accuracy digital maps are employed onboard to improve control accuracy, shorten travel time, and lower energy consumption [1], [2]. Environment sensing is a premise of autonomous

Manuscript received April 6, 2017; revised September 1, 2017; accepted October 19, 2017. Manuscript received in final form October 25, 2017. This work was supported in part by NSF China under Grant 51622504 and Grant 51575293, in part by the National Key Research and Development Program of China under Grant 2016YFB0100906, in part by the International Science and Technology Cooperation Program of China under Grant 2016YFE0102200, and in part by NSF USA Grant CNS-1647200 and Grant CNS-1054634. Recommended by Associate Editor A. Serrani. (Shengbo Eben Li and Xiaohui Qin contributed equally to this work) (Corresponding author: Keqiang Li.)

S. E. Li, X. Qin, J. Wang, and K. Li are with the State Key Laboratory of Automotive Safety and Energy, Tsinghua University, Beijing 100084, China (e-mail: lisb04@gmail.com; qxh880507@163.com; wjqlws@tsinghua.edu.cn; likq@tsinghua.edu.cn).

Y. Zheng is with the Department of Engineering Science, University of Oxford, OX1 3PJ, U.K. (e-mail: zhengy093@gmail.com).

H. Zhang is with the Department of Electrical and Computer Engineering, Iowa State University, Ames, IA 50011 USA (e-mail: hongwei@iastate.edu). Color versions of one or more of the figures in this paper are available online at http://ieeexplore.ieee.org.

Digital Object Identifier 10.1109/TCST.2017.2768041

control, which benefits transportation safety largely if participants can cooperate with each other. By utilizing wireless communication, a host vehicle can receive information from other participants such as pedestrian and road side equipment, enabling better awareness of potential dangers, and thus better decisions can be made [3], [4]. One important application of the cooperative systems is the vehicle platooning. Employing a shorter spacing compared to traditional adaptive cruise control (ACC) systems, platooning of connected vehicles has the potential to significantly increase traffic capacity [5]–[7] and reduce fuel consumption [8], [9].

The design of a platoon needs to consider three important performances, namely, internal stability, string stability, and scalability [10]. A platoon with linear time-invariant dynamics is internal stable if and only if all real parts of the eigenvalues of the closed-loop system are negative [11], [12], while the string stability requires the attenuation of spacing errors along the platoon [13]. Scalability represents the scaling trend of the stability margin of a platoon with the increase of its size [11]. These three performances are all closely related to traffic safety and smoothness, and have received intensive attention recently. Previous works usually focus on one of them; see [10], [16] for a recent review. Earlier platoon applications date back to the 1980s, which normally used the radars as their exclusive sensors to detect neighboring vehicles. Within this sensing framework, the nodes in a platoon can only acquire information from its immediate neighbors, i.e., the front and back ones. Consequently, the types of underlying communication topologies are quite limited, with predecessor following (PF) type [17], [18], and bidirectional PF (BPF) type [11], [19] as typical examples. The relationship between these configurationally simple topologies and string stability has been investigated by Ploeg et al. [14], Liang and Peng [18], Seiler et al. [20], and Middleton and Braslavsky [21], which have revealed certain essential limitations for rigid formation. Several approaches were proposed to improve string stability, such as adding communication links [7] and relaxing formation rigidity [22].

With the rapid development of wireless communication technologies [23], new topologies become available for platoon applications, for instance, leader PF (LPF), two-PF (TPF), and two-BPF (TBPF) [11]. However, only a few communication topologies have been fully studied in terms of their relationship with internal stability, string stability, and scalability. A well-known example is the platoon system

developed by the PATH program, where the leader's state is broadcasted to all the followers, resulting in a LPF topology [7]. Darbha and Rajagopal [24] studied the maximum spacing error of platoons with undirected topologies, and showed that it is necessary to have one vehicle linked to a large number of other vehicles to restrain the growth of spacing errors. Ploeg et al. [14] compared the string stability between PF topology and TPF topology under constant time-headway policy, and pointed out that TPF can yield a better string stability margin at a larger communication delay. Using the Routh-Hurwitz stability criterion, Zheng et al. [11] explicitly established the threshold of the linear feedback gains for communication topologies with real eigenvalues, and further compared the scalability of platoons under BPF topology and bidirectional LPF topology. In [6], two basic methods were proposed to improve the stability margin in terms of topology selection and control adjustment from a unified viewpoint. More recently, a distributed model predictive control algorithm was introduced for heterogeneous vehicle platoons in [25], which could guarantee internal stability for any unidirectional topologies. This diverse body of works has provided certain insights into the impact of different communication topologies on platoon performance.

The information exchange among vehicles enabled via wireless communication has the potential to improve platoon performances. However, network imperfections, such as timedelay and packet loss, may impair platoon performances, which need to be carefully addressed for practical applications. More recently, Bernardo et al. [41] modeled the platooning as a consensus problem, where time-varying heterogeneous delays were explicitly considered. Xiao and Gao [40] derived a minimum time-headway gaps to guarantee string stability for both homogenous and heterogeneous platoons, where the time delays of actuators and sensors were considered. In [38], a definition for heterogeneous string stability was proposed, and a necessary and sufficient condition for heterogeneous string stability was given for the constant spacing strategy. Note that heterogeneous platoons are often investigated under simple topologies such as PF and LPF; see [5], [14], [38], [40].

Despite some recent attention on topological varieties [5]–[7], [10], [24], [25], the types of topologies involved in previous studies are still rather limited, and most existing results are only applicable for the case where all the eigenvalues of the corresponding Laplacian matrix are real. To the best of our knowledge, the relationship between generic topologies and platoon internal stability is still unknown, especially when the Laplacian matrix contains complex eigenvalues. This paper studies the internal stability of a platoon under generic topologies with complex eigenvalues, proposes controller synthesis methods to find feasible control gains, and analyzes the error propagations. The vehicles in the platoon are assumed to share a three-order linear model achieved by an inverse model compensation, as used in [26]. A distributed linear feedback controller is designed considering the constant spacing policy. The main contributions of this paper are summarized as follows. First, a sufficient and necessary condition on the internal stability is derived for platoons under topologies with complex

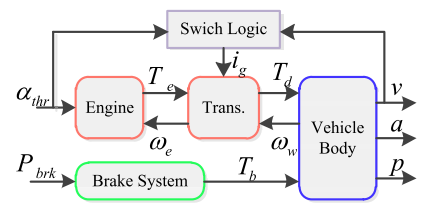


Fig. 1. Sketch of vehicle longitudinal dynamics.

eigenvalues. This result covers many previous studies that are only suitable for limited kind of topologies. In contrast to previous works [6], [11], [27], the condition provided in this paper is in real number field, facilitating the design of feedback gains subsequently. Second, by utilizing the proposed internal stability condition, a Riccati inequality based algorithm is proposed to compute the distributed feedback gain, which is decoupled from the communication topology. This makes the computation complexity independent of the platoon size, offering improvements over previous studies whose computation is scaling with platoon size [28], [29]. Third, we formulate the problem of disturbance propagation as an H_{∞} performance. By combining the Riccati inequality and Lyapunov analysis, an upper bound on the spacing errors of the platoon is provided. This result indicates that disturbance propagation is mainly determined by the topology structure, while the design of feedback gains only has a limited influence, which agrees with the results on the stability margin for platoons in [6] and [11].

The remainder of this paper is organized as follows. Section II presents the problem statement, including platoon configuration and modeling. Section III gives an internal stability theorem. The linear matrix inequality (LMI) based algorithm for controller synthesis is presented in Section IV. The results on disturbance propagation is presented in Section V. Simulation results demonstrate the effectiveness of this study in Section VI, and Section VII concludes the paper.

II. PROBLEM STATEMENT

A. Notations

Real and complex domains are denoted by \mathbb{R} and \mathbb{C} , respectively. $A \in R^{n \times m}$ denotes a real matrix of size $n \times m$. Given a square matrix A, we denote $He(A) = A + A^T$. $A \otimes B$ represents the Kronecker product between A and B of appropriate dimensions. Let Z be a complex matrix, then Z^* is its conjugate complex matrix. $\mathbf{1}_N$ denotes a column vector of size N with all its entries being 1. $e_{n,i} \in R^n$ is an n-dimensional column vector with all the elements being zero except for the ith entry being 1. Matrix A being Hurwitz means that every eigenvalue of A has strictly negative real part.

B. Model for Vehicle Dynamics

This study considers a platoon composed by a series of passenger cars. Each car is equipped with an internal combustion engine, an automatic transmission, and a hydraulic brake system. Only longitudinal dynamics are considered in the study, consisting of some nonlinear components, such as engine, transmission, aerodynamics, and tire slip. Fig. 1 demonstrates the sketch of vehicle longitudinal dynamics, where key

TABLE I
KEY PARAMETERS IN FIG. 1

Symbol	Meaning	
α_{thr}	Throttle input	
P_{brk}	Brake pressure	
T_e	Actual engine torque	
i_g	Gear ratio of transmission	
T_d	Driving torque on wheels	
T_b	Braking torque on wheels	
ω_e	Engine speed	
ω_w	Speed of the transmission output shaft	
v	Vehicle speed	
a	Vehicle acceleration	
p	Vehicle position	

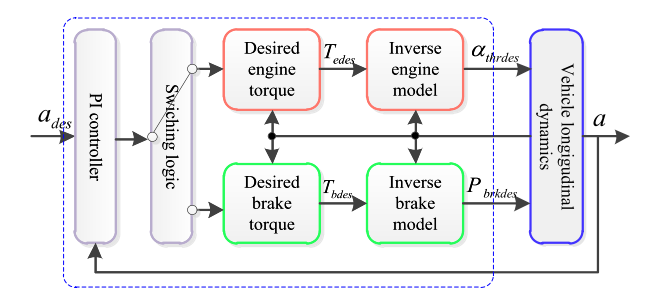


Fig. 2. Inverse model compensation.

parameters are explained in Table I. The inputs are throttle angle a_{thr} and brake pressure P_{brk} , and the outputs are the longitudinal acceleration a, velocity v, and position p [30].

To compensate for the salient nonlinearities introduced by engine static nonlinearity, torque converter coupling, discontinuous gear ratio, and quadratic aerodynamic drag, an inverse model compensation method is used. With the approach proposed in [11], shown in Fig. 2, the vehicle longitudinal dynamics can be approximated to the first-order inertial function depicted in (1), where $a_{\rm des}$ is the desired acceleration, a is the actual vehicle acceleration response, and τ_a is the inertial time delay

$$a(s) = \frac{a_{\text{des}}(s)}{\tau_a s + 1}.\tag{1}$$

Choose vehicle position p, velocity v, and acceleration a as the state variable, then a state space representation of the vehicle dynamics is derived in (2) as used in [6] and [11]

$$\dot{x} = Ax + Bu \tag{2}$$

where

$$x = \begin{bmatrix} p \\ v \\ a \end{bmatrix}, \quad A = \begin{bmatrix} 0 & 1 & 0 \\ 0 & 0 & 1 \\ 0 & 0 & -\frac{1}{\tau_a} \end{bmatrix}, \quad B = \begin{bmatrix} 0 \\ 0 \\ \frac{1}{\tau_a} \end{bmatrix}.$$

Remark 1: For conciseness and completeness, the linear model (4), which is obtained from the realistic model shown in Fig. 1 by using an inverse model compensation, is used in the following theoretical analysis. However, we shall employ a realistic model in simulations to validate the proposed methods. Note that this strategy has been widely adopted in [5], [6], [12], [14], and [15], where similar linear vehicle

models are used for theoretical analysis. The major difference lies in the techniques to simplify realistic vehicle dynamics; see [10], [16] for comprehensive discussions.

C. Closed-Loop Platoon Dynamics

A platoon is composed of N + 1 vehicles, including one leader and N followers. The leader is indexed by 0, and the followers are numbered as $1, 2, \ldots, N$, consecutively

The communication topology is modeled by a directed graph $\mathcal{G} = (V, E)$, which is widely used in the multiagent control community[31]–[34]. The topological connectivity of the platoon is included in \mathcal{G} , which is depicted by a set of nodes $V = \{1, 2, ..., N\}$ and a set of edges $\varepsilon \subseteq V \times V$. The connectivity between two nodes are denoted by an adjacency matrix $M = [m_{ij}] \in \mathbb{R}^{N \times N}$, with entries $m_{ij} > 0$, if $(j, i) \in \varepsilon$ (i.e., node i receives information from node j), and $m_{ij} = 0$, if $(j, i) \notin \varepsilon$. In this paper, equal weights are adopted, resulting in the adjacency matrix definition shown in (3). Note that no self-loop is permitted in a platoon, i.e., $(i, i) \notin \varepsilon$

$$\begin{cases}
 m_{ij} = 1, i f(j, i) \in \varepsilon \\
 m_{ij} = 0, i f(j, i) \notin \varepsilon.
\end{cases}$$
(3)

The Laplacian matrix associated with \mathcal{G} is defined as $L_G = [l_{ij}] \in \mathbb{R}^{N \times N}$, where

$$\begin{cases} l_{ij} = -m_{ij}, & \text{if } i \neq j \\ l_{ii} = \sum_{k=1}^{N} m_{ik}, & \text{if } i = j. \end{cases}$$

$$(4)$$

To describe the connectivity between the leader and followers, a pinning matrix is defined

$$P_G = \begin{bmatrix} p_{G1} & & \\ & \ddots & \\ & & p_{GN} \end{bmatrix}$$
 (5)

where $p_{Gi} = 1$, if node *i* receives information from the leader, and $p_{Gi} = 0$, otherwise. Note that the combination of Laplacian matrix and pinning matrix determines the characteristics of the communication topology.

The objective of platoon control is to track the leading speed, and maintain a desired spacing between two consecutive followers. For node i, its desired state is

$$\begin{cases} v_i = v_0 \\ p_i = p_{i-1} - d_{i,i-1} \end{cases}$$
 (6)

where $d_{i,j}$ is the desired spacing between vehicle i and vehicle j. Here, $d_{i,j}$ is determined by a constant spacing policy, which has the potential to increase the traffic capacity and fuel efficiency [11], [15]. The relationship shown in (6) can be further written in a compact form

$$x_i = x_{i-1} - D_{i,i-1} (7)$$

where

$$D_{i,i-1} = \begin{bmatrix} d_{i,i-1} \\ 0 \\ 0 \end{bmatrix}.$$

The feedback controller is linear and distributed in a form as

$$u_i = K \sum_{j=1}^{N} (l_{ij}(x_j - x_i - D_{i,j})) + K p_{Gi}(x_0 - x_i - D_{i,0})$$
 (8)

where

$$K = (k_1 \ k_2 \ k_3) \tag{9}$$

is the static feedback gain, l_{ij} is the entry of Laplacian matrix, and p_{Gi} is the entry of the pinning matrix. The tracking error of node i with respect to the leader is expressed as

$$\tilde{x}_i = x_0 - x_i - D_{i,0}. \tag{10}$$

It can be verified that $AD_{i,0} = 0$ and $D_{i,j} = D_{i,0} - D_{j,0}$. Differentiating (10) on both sides and substituting (2) into it, a linear model of the closed-loop platoon dynamics is obtained

$$\dot{\tilde{x}}_{i} = A\tilde{x}_{i} + BK \sum_{j=1}^{N} (l_{ij}(\tilde{x}_{j} - \tilde{x}_{i})) + BK p_{Gi}(\tilde{x}_{0} - \tilde{x}_{i}) + Bu_{0}$$
 (11)

where u_0 is the control input of the leading vehicle. Define a collective state including all the followers as

$$\tilde{X} = \left[\tilde{x}_1^T \cdots \tilde{x}_N^T \right]^T. \tag{12}$$

Then all the dynamics of the followers can be rewritten as

$$\dot{\tilde{X}} = [I_N \otimes A - H \otimes (BK)] \tilde{X} + (\mathbf{1}_N \otimes B) u_0$$
 (13)

where $H = (L_G + P_G)$.

As is shown in (13), the internal stability is affected not only by the vehicle dynamics and the feedback gain, but also by the communication topology. All the vehicles in the platoon are interconnected through the communication topology. Each topology corresponds to a unique *H* matrix. Note that ideal communication network is assumed in this work, *i.e.*, no communication delay or packet loss is considered.

III. INTERNAL STABILITY WITH GENERIC COMMUNICATION TOPOLOGIES

A platoon with linear time-invariant dynamics is internally stable if and only if all the eigenvalues of the closed-loop system have negative real parts [11]. We derive a sufficient and necessary condition for a stable platoon with generic communication topologies in this section.

A. Eigenvalues of H Matrix

The properties of the eigenvalues of H greatly influence the internal stability of a platoon. Here, we briefly discuss the eigenvalues of H before presenting the stability analysis.

The eigenvalues of H can be complex with arbitrary multiplicity even though H is a real matrix. Two kinds of real matrices are known to only have real eigenvalues: 1) symmetric matrix and 2) triangular matrix [11]. For an arbitrary matrix which is neither symmetric nor triangular, it is not easy to decide whether it contains complex eigenvalues. Table II lists the properties of six H matrices corresponding to different communication topologies, namely, PF, BPF, TPF, TBPF, two predecessor single following (TPSF), single predecessor two

TABLE II PROPERTIES OF TYPICAL TOPOLOGIES

Topology	<i>H</i> Matrix	Complex Eigenvalue	Number of Different Eigenvalues
PF	H_{PF}	No	1
BPF	H_{BPF}	No	N
TPF	H_{TPF}	No	1
TBPF	H_{TBPF}	No	N
TPSF	H_{TPSF}	Yes	N
SPTF	H_{SPTF}	Yes	N
Mix	H_{Mix}	Yes	N

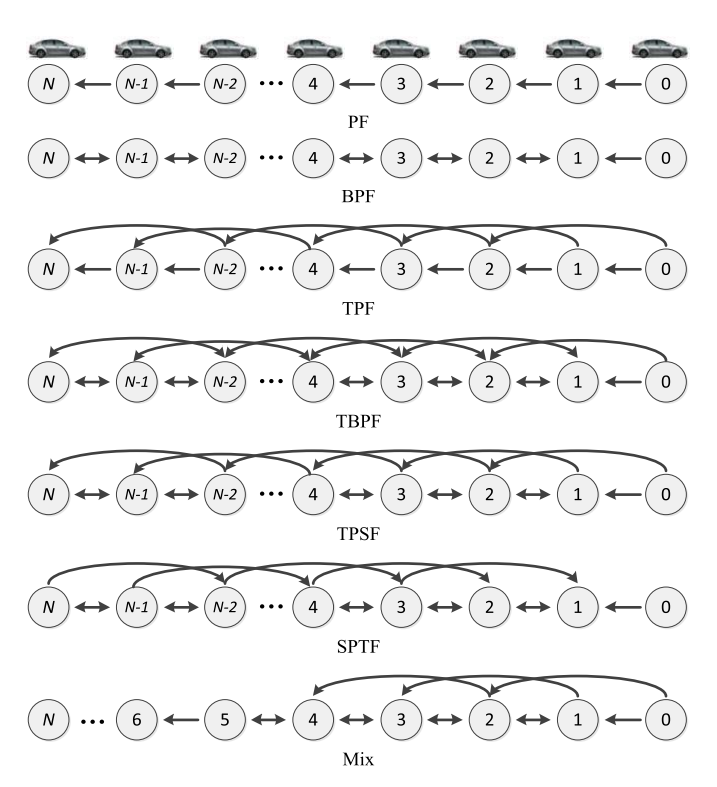


Fig. 3. Typical communication topologies.

following (SPTF), and a mixed topology. Since the first four types are well-known (see [11] for details), their H matrices are not listed here for brevity. These topologies are demonstrated in Fig. 3. The H matrices of the first four topologies have special structures with real eigenvalues, while the last three types contain complex eigenvalues. In fact, the $H_{\rm Mix}$ is a combination of $H_{\rm TPSF}$ and $H_{\rm PF}$, indicating that a small change on topologies with real eigenvalues would result in topologies with complex eigenvalues.

Where

$$H_{\text{TPSF}} = \begin{bmatrix} 2 & -1 \\ -1 & 3 & -1 \\ -1 & -1 & 3 & -1 \\ & \ddots & \ddots & \ddots \\ & & -1 & -1 & 3 & -1 \\ & & & -1 & -1 & 2 \end{bmatrix}$$

LI et al.: DISTRIBUTED PLATOON CONTROL UNDER TOPOLOGIES

$$H_{\text{SPTF}} = \begin{bmatrix} 3 & -1 & -1 & & & \\ -1 & 3 & -1 & \ddots & & \\ & -1 & 3 & \ddots & -1 & \\ & & -1 & \ddots & -1 & -1 \\ & & & \ddots & 2 & -1 \\ & & & & -1 & 1 \end{bmatrix}$$

$$H_{\text{Mix}} = \begin{bmatrix} 2 & -1 & & & & \\ -1 & 3 & -1 & & & \\ -1 & -1 & 3 & -1 & & \\ & & & -1 & 1 & \\ & & & & \ddots & \ddots & \\ & & & & & -1 & 1 \end{bmatrix}.$$

B. Stability Analysis

Lemma 1 [35]: Let H be an arbitrary square matrix of size N, λ_i , i = 1, 2, ..., q be the real eigenvalues of H including multiplicity, and $\lambda_i = \sigma_i + j\omega_i$, $\lambda_i^* = \sigma_i - j\omega_i$, i = q + 1, $q+2,\ldots,q+r$ be the conjugate complex eigenvalues of H including multiplicity. Then there exists a nonsingular matrix $V \in \mathbb{R}^{N \times N}$, such that

$$\begin{cases}
V^{-1}HV = J \in \mathbb{R}^{N \times N} \\
J_1 & \ddots & & \\
& J_q & & \\
& & J_{q+1} & & \\
& & & \ddots & \\
& & & & J_{q+r}
\end{cases}$$
(14)

where J_i , i = 1, 2, ..., q are the same as the diagonal subblocks of the Jordan canonical form of H corresponding to the real eigenvalues, which have the form

$$J_{i} = \begin{bmatrix} \lambda_{i} & 1 & & & \\ & \lambda_{i} & \ddots & & \\ & & \ddots & 1 & \\ & & & \lambda_{i} & \end{bmatrix}, \quad i = 1, 2, \dots, q. \quad (15) \quad \text{where}$$

The remaining diagonal subblocks have the following form:

$$\begin{cases} J_i = \begin{bmatrix} S_i & I_2 & & & & \\ & S_i & \ddots & & \\ & & \ddots & I_2 \\ & & & S_i \end{bmatrix} &, \quad i = q+1, \dots, q+r \quad (16) \end{cases}$$
 values are
$$\begin{bmatrix} \Psi_l & I_2 \otimes (BK) & & & \\ & \Psi_l & \ddots & & \\ & & \ddots & I_2 \otimes (BK) \\ & & & \ddots & I_2 \otimes (BK) \end{bmatrix}$$
 where

whose sizes are two times of the diagonal subblocks of the Jordan canonical form of H corresponding to the complex eigenvalues $\lambda_i = \sigma_i + j\omega_i$, $i = q + 1, q + 2, \dots, q + r$. Let n_i

be the size of J_i , i = 1, 2, ..., q + r, then

$$\sum_{i=1}^{q+r} n_i = N. \tag{17}$$

Remark 2: The result in Lemma 1 equivalently converts an arbitrary square matrix into a canonical form without changing eigenvalues, which offers convenience for the subsequent stability analysis.

We are now ready to present the first theorem on internal stability.

Theorem 1: Let λ_i , $i = 1, 2, \dots, q$ be the real eigenvalues of H including multiplicity, and $\lambda_i = \sigma_i + j\omega_i, \lambda_i^* = \sigma_i$ $j\omega_i$, $i=(q+1), (q+2), \ldots, (q+r)$ be the conjugate complex eigenvalues including multiplicity. For a homogeneous linear platoon described by (13), the platoon is internally stable if and only if the following matrices are Hurwitz:

$$\begin{cases} A - \lambda_i BK, & i = 1, \dots, q \\ I_2 \otimes A - \begin{bmatrix} \sigma_i & \omega_i \\ -\omega_i & \sigma_i \end{bmatrix} \otimes (BK), & i = q + 1, \dots, q + r. \end{cases}$$
(18)

Proof: Internal stability requires the following condition:

$$(I_N \otimes A - H \otimes (BK))$$
 is Hurwitz. (19)

According to Lemma 1, there exists a nonsingular transformation matrix V, such that $V^{-1}HV = J$, where J is the canonical form of H. Then, we have the following similarity transformation:

$$(V^{-1} \otimes I_3)(I_N \otimes A - H \otimes (BK))(V \otimes I_3)$$

= $I_N \otimes A - J \otimes (BK)$. (20)

Due to the structure of J, the resulting matrix $[I_N \otimes A J \otimes (BK)$] is a block diagonal matrix. In particular, the main diagonal blocks corresponding to real eigenvalues λ_i is are

$$\begin{bmatrix}
\Phi_i & BK \\
& \Phi_i & \ddots \\
& & \ddots & BK \\
& & \Phi_i
\end{bmatrix}$$
(21)

$$\begin{cases}
\Phi_i = A - \lambda_i BK \\
\lambda_i \in \mathbb{R}
\end{cases} i = 1, 2, \dots, q.$$
(22)

The main diagonal blocks corresponding to complex eigenvalues are

$$\begin{bmatrix}
\Psi_l & I_2 \otimes (BK) \\
& \Psi_l & \ddots \\
& & \ddots & I_2 \otimes (BK) \\
& & & \Psi_l
\end{bmatrix} (23)$$

where

$$\begin{cases}
\Psi_l = I_2 \otimes A - \begin{bmatrix} \sigma_l & \omega_l \\ -\omega_l & \sigma_l \end{bmatrix} \otimes (BK) \\
\lambda_l = \sigma_l + j\omega_l, (q+1) \leq l \leq (q+r).
\end{cases}$$
(24)

It is easy to know that the eigenvalues of the submatrices (21) and (23) are determined by Φ_i and Ψ_l , respectively

$$eig(I_N \otimes A - H \otimes (BK))$$

$$= eig(I_N \otimes A - J \otimes (BK))$$

$$= \left(\bigcup_{i=1}^q eig(\Phi_i)\right) \cup \left(\bigcup_{l=q+1}^r eig(\Psi_l)\right). \tag{25}$$

Thus, the condition (19) holds if and only if

$$\begin{cases}
\Phi_i \text{ is Hurwitz, } i = 1, \dots, q \\
\Psi_l \text{ is Hurwitz, } l = (q+1), \dots, (q+r)
\end{cases}$$
(26)

which is equivalent to (18), and this completes the proof.

We note that the result of Theorem 1 is applicable for general linear time-invariant dynamics, in addition to the vehicle model (2). Our following results will directly depend on the vehicle dynamics.

Remark 3: If H has only real eigenvalues, then the conditions in

Theorem 1 will be reduced to: $(A - \lambda_i BK)$ being Hurwitz, i = 1, 2, ..., N, which has been reported in [11] for the stability analysis of platoon control. However, the results in [11] fail to deal with complex eigenvalues. Here, the results in Theorem 1 can cover general cases. Besides, the condition (18) is in real number domain, even if the communication topology contains complex eigenvalues. This offers conveniences for further controller synthesis.

Remark 4: If H has zero eigenvalues, then stability requires A to be Hurwitz, which is actually infeasible for the vehicle model (2). Thus, a necessary condition to guarantee the internal stability is $\det(H) \neq 0$. As shown in

Theorem 1, the influence of communication topology on internal stability is reflected by the eigenvalues of H. A better topology will ensure a larger stability margin, which can be exploited for other system performance design (see a recent result [6] for details).

IV. CONTROLLER SYNTHESIS

This section introduces two algorithms to calculate the static state feedback gain *K* based on the Riccati inequality. We first present a method to calculate a stable feedback gain, and then further propose a way to design a controller with a guaranteed convergence speed. The following lemmas are needed before preceding to the main theorems.

Lemma 2[35]: Given $Q = [q_{ij}] \in \mathbb{R}^{N \times N}$, then all the eigenvalues of Q are located in the union of the N disks

$$\bigcup_{i=1}^{N} \left\{ z \in \mathbb{C} \, | \, |z - q_{ii}| \le \sum_{j=1, j \ne i}^{N} |q_{ij}| \right\}. \tag{27}$$

Lemma 3 [36]: Given $A \in \mathbb{R}^{N \times N}$, then A is Hurwitz if and only if there exists a positive definite matrix P > 0, such that

$$He(AP) < 0. (28)$$

The following theorem provides a sufficient condition to solve the distributed control gain.

Theorem 2: For a homogeneous platoon under node model (2) using control law (8), and given λ_i , $1 \le i \le q + r$, as the eigenvalues of H, then we have the following.

1) A necessary condition to ensure internal stability is that there exists a positive real number μ satisfying

$$0 < \mu \le \frac{\lambda_i + \lambda_i^*}{2}, \quad 1 \le i \le q + r. \tag{29}$$

2) If there exists a positive definite matrix Q > 0, such that

$$He(QA) - \mu QBB^T Q < 0. (30)$$

then there exists a control law (8) which guarantees the internal stability of the platoon system (13), and the feasible static control gain K can be constructed as

$$K = \frac{1}{2}B^T Q. (31)$$

Proof: As for the first statement, the definition of H makes it a diagonally dominant matrix, *i.e.*,

$$|h_{ii}| \ge \sum_{j=1, j \ne i}^{N} |h_{ij}|, \quad i = 1, \dots, N$$
 (32)

where h_{ij} , $1 \le i, j \le N$ are the entries of the matrix H. The definition of H guarantees that $h_{ii} > 0$. For the disks defined in (27), the following inequality holds:

$$z \ge h_{ii} - \sum_{j=1, j \ne i}^{N} |h| \ge 0.$$
 (33)

Therefore, all the disks defined in (27) are located in the closed right half-plane. Then, for any eigenvalue, λ_i , $1 \le i \le q + r$, we have

$$0 \le \frac{\lambda_i + \lambda_i^*}{2}, \quad 1 \le i \le q + r \tag{34}$$

where the equality holds only if $\lambda_i = 0$ [since the region proposed by (27) is a circle, zero can be reached only if $\lambda_i = 0$].

If zero is an eigenvalue of H, then from Theorem 1, A must be Hurwitz, which in fact cannot be satisfied. Therefore, all the eigenvalues of H have positive real parts, thus inequality (34) can be strengthened to

$$0 < \frac{\lambda_i + \lambda_i^*}{2}, \quad 1 \le i \le q + r. \tag{35}$$

Thus, a necessary condition is that there exists a positive real number μ satisfying (29).

Next, we shall show that the control gain K (31) stabilizes the platoon system. To this end, let μ_0 be a real positive number and $P_0 = Q^{-1}$ be a symmetric matrix satisfying (29) and (30), respectively. Internal stability requires to the condition (18). Without loss of generality, let H contain both real eigenvalues and complex eigenvalues.

For real eigenvalues, *i.e.*, λ_i , $i = 1, 2, \dots, q$, from Lemma 3, we know internal stability holds if and only if there exist matrices $P_i > 0$, $i = 1, 2, \dots, q$, such that

$$He[(A - \lambda_i BK)P_i] < 0, \quad 1 < i < q + r.$$
 (36)

Let
$$P_i = P_0, i = 1, 2, ..., q$$
, and $K = (B^T P_0^{-1})/2$. Then
$$He[(A - \lambda_i B K) P_i]$$

$$= He \left[\left(A - \lambda_i B \frac{B^T P_0^{-1}}{2} \right) P_0 \right]$$

$$= He(AP_0) - \lambda_i B B^T. \tag{37}$$

Since inequality (29) holds, combining (30) yields

$$He[(A - \lambda_i BK)P_i] = He(AP_0) - \lambda_i BB^T$$

$$\leq He(AP_0) - \mu_0 BB^T$$

$$< 0. \tag{38}$$

Thus, the condition (36) is satisfied.

For complex eigenvalues $\lambda_i = \sigma_i + \omega_i$, i = (q+1), $(q+2), \dots, (q+r)$, internal stability holds if and only if there exist matrices $\tilde{P}_i > 0$, $(q+1) \le i \le (q+r)$, such that

$$He\left\{\left[I_{2}\otimes A-\begin{bmatrix}\sigma_{i}&\omega_{i}\\-\omega_{i}&\sigma_{i}\end{bmatrix}\otimes(BK)\right]\tilde{P}_{i}\right\}<0. \quad (39)$$

Set $\tilde{P}_i = I_2 \otimes P_0$, and $K = (B^T P_0^{-1})/2$. Then

$$He\left\{\left[I_{2}\otimes A - \begin{bmatrix}\sigma_{i} & \omega_{i} \\ -\omega_{i} & \sigma_{i}\end{bmatrix}\otimes (BK)\right]\tilde{P}_{i}\right\}$$

$$= He\left\{\left[I_{2}\otimes A - \begin{bmatrix}\sigma_{i} & \omega_{i} \\ -\omega_{i} & \sigma_{i}\end{bmatrix}\otimes \left(B\frac{B^{T}P_{0}^{-1}}{2}\right)\right](I_{2}\otimes P_{0})\right\}$$

$$= He\left[I_{2}\otimes (AP_{0})\right] - He\left\{\begin{bmatrix}\sigma_{i} & \omega_{i} \\ -\omega_{i} & \sigma_{i}\end{bmatrix}\otimes \left(\frac{BB^{T}}{2}\right)\right\}$$

$$= He\left[I_{2}\otimes (AP_{0})\right] - I_{2}\otimes (\sigma_{i}BB^{T})$$

$$- He\left\{\begin{bmatrix}0 & \omega_{i} \\ -\omega_{i} & 0\end{bmatrix}\otimes \left(\frac{BB^{T}}{2}\right)\right\}. \tag{40}$$

Here, since BB^T is symmetric, thus

$$He\left\{ \begin{bmatrix} 0 & \omega_i \\ -\omega_i & 0 \end{bmatrix} \otimes \left(\frac{BB^T}{2} \right) \right\} = 0. \tag{41}$$

Substituting (41) into (40), we have

$$He \left\{ \begin{bmatrix} I_2 \otimes A - \begin{bmatrix} \sigma_i & \omega_i \\ -\omega_i & \sigma_i \end{bmatrix} \otimes (BK) \end{bmatrix} \tilde{P}_i \right\}$$

$$= He[I_2 \otimes (AP_0)] - I_2 \otimes (\sigma_i BB^T)$$

$$= I_2 \otimes [He(AP_0) - \sigma_i BB^T]$$

$$\leq I_2 \otimes [He(AP_0) - \mu_0 BB^T]$$

$$< 0. \tag{42}$$

The last two inequalities hold due to the satisfaction of (29) and (30). Therefore, the condition (39) holds.

From Theorem 1, (36) and (39) guarantees the internal stability defined by Theorem 2, and (31) is one of the feasible controllers. This completes the proof.

Riccati matrix inequality (30) is the key to Theorem 2. As long as this LMI can be solved, a feasible control gain can be formulated through (31). The influence of communication topology is decoupled by the parameter μ , which should be no larger than any real part of the eigenvalues. Therefore, the computation complexity is independent of the platoon size. This fact offers us benefits compared to previous studies whose computation burden is scaling with platoon size; see [28], [29].

Remark 5: When there exists an eigenvalue close to the imaginary axis, the resulting feedback gain will become numerically large. This is inevitable for such communication topologies, which can be viewed as certain essential limitations [6]. Since the feedback gain influences the system dynamics through topology eigenvalues in (18), a smaller real part amount to a weaker influence, leading to the requirement that the feedback gain must be large enough to stabilize the system. This fact agrees with the results in [6] and [11]. We note that since (A, B) is controllable, the control gain in Theorem 2 can always be solved. In other words, for a homogeneous platoon with node model (2) and control law (8), the existence of a stabilizing control gain K is equivalent to $\det(H) \neq 0$.

Theorem 2 provides an approach to find the stabilizing control gain. One drawback is that there is no guarantee for the convergence speed of spacing errors. A long convergence time may be intolerable in real applications. To address this issue, the following theorem is proposed.

Theorem 3: For a homogeneous platoon with node model (2) and control law (8). Let μ be the positive scalar defined in Theorem 2, if there exists a positive scalar δ and a symmetric matrix P > 0, such that

$$He(AP) - \mu BB^T + 2\delta P < 0 \tag{43}$$

then the spacing errors converge to zero exponentially faster than $exp(-\delta t)$ with the control gain defined by (31).

Proof: With the control gain defined by (31), similar to the proof of Theorem 2, the following two conditions can be verified:

$$He((A - \lambda_i BK + \delta I_3)P)$$

$$= He(AP) - \lambda_i BB^T + 2\delta P$$

$$\leq He(AP) - \mu BB^T + 2\delta P$$

$$< 0$$
(44)

and

$$He((I_{2} \otimes A - \begin{bmatrix} \sigma_{i} & \omega_{i} \\ -\omega_{i} & \sigma_{i} \end{bmatrix}) \otimes (BK) + \delta I_{6})(I_{2} \otimes P))$$

$$= He[I_{2} \otimes (AP_{0})] + 2\delta I_{2} \otimes P - I_{2} \otimes (\sigma_{i}BB^{T})$$

$$- He\left\{\begin{bmatrix} 0 & \omega_{i} \\ -\omega_{i} & 0 \end{bmatrix} \otimes \left(\frac{BB^{T}}{2}\right)\right\}$$

$$= I_{2} \otimes \left[He(AP_{0}) - \sigma_{i}BB^{T} + 2\delta P\right]$$

$$\leq I_{2} \otimes \left[He(AP_{0}) - \mu BB^{T} + 2\delta P\right]$$

$$< 0. \tag{45}$$

With (25) and Lemma 3, it is obvious that

$$(I_N \otimes A - H \otimes (BK) + \delta I_{3N})$$
 is Hurwitz. (46)

Define a symmetric matrix $\bar{P} = (I_N \otimes P) \in S^{3N \times 3N} > 0$. Then we have

$$He(\bar{P}(I_N \otimes A - H \otimes (BK) + \delta I_{3N})) < 0.$$
 (47)

Choose a Lyapunov function as $V_E = \tilde{X}^T \bar{P} \tilde{X} > 0$, then

$$\dot{V}_E = \tilde{X}^T (He(\bar{P}(I_N \otimes A - H \otimes (BK))))\tilde{X}
< -2\delta \tilde{X}^T \bar{P} \tilde{X}
= -2\delta V_F.$$
(48)

According to the well-known Comparison lemma [36], it is obtained from (48) that $V_E(t) < e^{-2\delta t} V_E(00)$. Then

$$\lambda_{\min}(P) \|\tilde{X}(t)\|_{2}^{2} \leq V_{E}(t) < e^{-2\delta t} V_{E}(0)$$

$$\leq \lambda_{\max}(P) \|\tilde{X}(0)\|_{2}^{2}. \tag{49}$$

Therefore, it yields

$$\left\|\tilde{X}(t)\right\|_{2} < e^{-\delta t} \left\|\tilde{X}(0)\right\|_{2} \sqrt{\lambda_{\max}(P)} / \lambda_{\min}(P). \tag{50}$$

Since the state variable \tilde{X} is composed by tracking errors, the condition (50) indicates that spacing errors converge to zero exponentially with a speed no slower than $exp(-\delta t)$.

Theorem 3 guarantees a better convergence speed at the price of worse solvability. A demand of large convergence speed may result in the infeasibility of the proposed LMI condition.

V. DISTURBANCE PROPAGATION

In addition to internal stability, robustness with respect to external disturbances is another important performance measure for platoons, which is also known as disturbance propagation. A commonly studied disturbance propagation is the uniform string stability (see [5], [7], [14], [18], [22]), which requires a uniform attenuation of spacing errors along the platoon. However, when various communication topologies are involved, uniform string stability is difficult to analyze theoretically. Similar to the approach proposed by Shaw and Hedrick [38], we do not expect the disturbance on the leader to attenuate uniformly along the string. Instead, we require bounded spacing errors of the followers when there exist bounded disturbances on the leader.

Since the state variable of the closed-loop platoon dynamics consist of spacing errors, the performance of disturbance propagation can be represented by the following bound:

$$\left\| \tilde{X}/\omega_0 \right\|_{\infty} < \gamma_{\rho} \tag{51}$$

where ω_0 is the disturbance on the input of the leader. To take the disturbance into account, we rewrite the closedloop dynamics as

$$\dot{\tilde{X}} = [I_N \otimes A - H \otimes (BK)] \tilde{X} + (I_N \otimes B)\omega$$
 (52)

where $\omega = \mathbf{1}_N \otimes \omega_0$.

The following theorem provides a controller synthesis method considering both internal stability and disturbance propagation performance.

Theorem 4: For a homogeneous platoon with node model (2) and control law (8). Let μ be defined in Theorem 2, and P_H be a positive definite solution of (53), if there exist two scalars $r_A > 0$ and $\rho > 0$ such that LMI (54) has a positive definite solution P, then the distributed control gain (55) stabilizes the platoon with a disturbance propagation bound expressed by (56)

$$P_H H + H^T P_H - 2\mu P_H > 0 (53)$$

$$\begin{bmatrix}
P_H H + H^T P_H - 2\mu P_H > 0 & (53) \\
He(AP) + (1 - r_A)BB^T & P \\
P & -1/\rho
\end{bmatrix} < 0$$
(54)

$$K = \frac{1}{\mu} r_A B^T P^{-1} \qquad (55)$$

$$\|\tilde{X}/\omega\|_{\infty} < \gamma_{\rho} = \sqrt{\frac{\lambda_{\max}(P_H)}{\rho \lambda_{\min}(P_H)}}.$$
 (56)

Proof: Theorem 4 holds if and only if the following two statements hold [39].

- 1) Internal stability is guaranteed when $\omega \equiv 0$.
- For zero initial conditions, the following inequality is satisfied:

$$\int_{t=0}^{+\infty} \|\tilde{X}(t)\|_{2}^{2} dt < \gamma_{\rho}^{2} \int_{t=0}^{+\infty} \|\omega(t)\|_{2}^{2} dt.$$
 (57)

To prove these two statements, the following Lyapunov function is chosen:

$$V = \tilde{X}^T (P_H \otimes P_A) \tilde{X} > 0 \tag{58}$$

where $P_A = P^{-1}$ is defined for conciseness in the following

For the first statement, since $\omega \equiv 0$, then it follows that:

$$\dot{V} = \tilde{X}^T He[P_H \otimes (P_A A) - (P_H H) \otimes (P_A B K)] \tilde{X}
= \tilde{X}^T \{P_H \otimes [He(P_A A) - r_A P_A B B^T P_A]\} \tilde{X}
- \tilde{X}^T \left[\frac{1}{\mu} (He(P_H H) - 2\mu P_H) \otimes (r_A P_A B B^T P_A) \right] \tilde{X}
< \tilde{X}^T \{P_H \otimes [He(P_A A) - r_A P_A B B^T P_A]\} \tilde{X}.$$
(59)

Based on Schur lemma, LMI (54) can be transformed into

$$He(P_AA) + (1-r_A)P_ABB^TP_A + \rho I < 0$$
 (60)

which guarantees \dot{V} < 0. Thus, the internal stability is

For the second statement, it is equivalent to proving

$$\int_{t=0}^{+\infty} \left[\tilde{X}^T \tilde{X} - \gamma_\rho^2 \omega^T \omega \right] dt$$

$$< \frac{1}{\rho \lambda_{\min}(P_H)} \left[V(t) |_0^{+\infty} - \int_{t=0}^{+\infty} \dot{V}(t) dt \right] (61)$$

which is guaranteed by

$$\rho \lambda_{\min}(P_H) (\tilde{X}^T \tilde{X} - \gamma_{\rho}^2 \omega^T \omega) + \dot{V} < 0.$$
 (62)

Differentiating the Lyapunov function along the system dynamics yields

$$\dot{V} = He[\tilde{X}^{T}(P_{H} \otimes P_{A})(I \otimes B)\omega]
+ \tilde{X}^{T}He[P_{H} \otimes (P_{A}A)]\tilde{X}
- \tilde{X}^{T}He\left[(P_{H}H) \otimes \left(\frac{r_{A}}{\mu}P_{A}BB^{T}P_{A}\right)\right]\tilde{X}.$$
(63)

For the first term in (63), the following inequality holds:

$$He\big[\tilde{X}^{T}(P_{H}\otimes P_{A})(I\otimes B)\omega\big] \\ \leq \tilde{X}^{T}[P_{H}\otimes (P_{A}BB^{T}P_{A})]\tilde{X} + \lambda_{\max}(P_{H})\omega^{T}\omega. \tag{64}$$

To prove (64), we rewrite it into the following form:

$$\begin{bmatrix} \tilde{X} \\ \omega \end{bmatrix}^T \begin{bmatrix} P_H \otimes (P_A B B^T P_A) & -P_H \otimes (P_A B) \\ -P_H \otimes (B^T P_A) & \lambda_{max}(P_H) \end{bmatrix} \begin{bmatrix} \tilde{X} \\ \omega \end{bmatrix} \ge 0.$$
(65)

With Schur lemma, (65) holds if and only if

$$\left(P_H - \frac{1}{\lambda_{\max}(P_H)} P_H P_H\right) \otimes (P_A B B^T P_A) \ge 0 \quad (66)$$

which is congruent with inequality as the following equation:

$$\left(P_H^{-1} - \frac{1}{\lambda_{\max}(P_H)}I_N\right) \otimes (P_A B B^T P_A) \ge 0. \tag{67}$$

Since λ $(P_H^{-1}) = 1/\lambda(P_H)$, inequality (67) obviously holds, so does (64). Substitute (56), (63), and (64) into (62), we have

$$\rho \lambda_{\min}(P_{H})[\tilde{X}^{T}\tilde{X} - \gamma_{\rho}^{2}\omega^{T}\omega] + \dot{V} \\
\leq \rho \tilde{X}^{T}(P_{H} \otimes I)\tilde{X} - \lambda_{\max}(P_{H})\omega^{T}\omega + \dot{V} \\
\leq \tilde{X}^{T}[P_{H} \otimes (He(P_{A}A) + \rho I + (1-r_{A})P_{A}BB^{T}P_{A}]\tilde{X} \\
- \frac{r_{A}}{\mu}\tilde{X}^{T}[(He(P_{H}H) - \mu P_{H}) \otimes (P_{A}BB^{T}P_{A})]\tilde{X} \\
\leq \tilde{X}^{T}[P_{H} \otimes (He(P_{A}A) + \rho I + (1-r_{A})P_{A}BB^{T}P_{A}]\tilde{X} \\
< 0. \tag{68}$$

Therefore, the second statement holds. This completes the proof.

Theorem 4 provides a method to analyze the disturbance propagation for generic communication topology. Note that inequality (53) is not a constraint on the control gain. As long as $det(H) \neq 0$, this inequality can be solved to find a positive definite matrix P_H . Inequality (54) is consistent with (43) in Theorem 3, which can be transformed into each other with proper tuning. The control gain given by (55) is also consistent with the one proposed previously. If $r_A = \mu/2$ is chosen, the control gain provided by (55) will be just the same to (31).

In addition, Theorem 4 gives a bound of the overall tracking errors when bounded input disturbance is applied to the leader in a platoon. The bound γ_{ρ} is determined by two terms, i.e., the eigenvalues of P_H , and the positive scalar ρ . The eigenvalues of P_H represent the influence from the intrinsic property of the communication topology on the platoon performance. A better topology can yield a smaller ratio between $\lambda_{\max}(P_H)$ and $\lambda_{\min}(P_H)$, which will lead to a lower bound γ_{ρ} . A larger choice of ρ can also yield a lower bound, but this would restrict the feasibility of LMI (54), which often results in a numerically large control gain K.

Remark 6: For symmetric topologies, i.e., $H = H^T$, the bound can be further improved to (69), where the eigenvalues of H are directly involved, which is much more convenient for numerical calculations

$$\gamma_{\rho} = \sqrt{\frac{\lambda_{\max}(H)}{\rho \lambda_{\min}(H)}}.$$
 (69)

Remark 7: The bound provided by Theorem 4 does not have a connection with platoon size explicitly, but this does not mean γ_{ρ} will not scale with platoon size. For a badly designed topology H, the ratio $\lambda_{\max}(P_H)/\lambda_{\min}(P_H)$ may increase together with platoon size, such as topology PF, BPF. Yet for some topologies, this ratio can be bounded by a constant upper limit, such as leader BPF(LBPF) type. The bound γ_{ρ} is mainly determined by the structure of H, the control gain design can influence γ_{ρ} through ρ only to a limited extent.

When investigating disturbance propagation, relative spacing error is often employed by literature, i.e.,

$$\bar{x}_i = x_{i-1} - x_i - D_{i,i-1}. \tag{70}$$

Unlike the previously defined \tilde{x}_i , relative spacing error is more concerned about local situation. Similarly, define a collective variable $\bar{X} = [\bar{x}_1^T \cdots \bar{x}_N^T]^T$, then we have

$$\bar{X} = (U \otimes I_3)\tilde{X} \tag{71}$$

where

$$U = \begin{bmatrix} 1 \\ -1 & 1 \\ & \ddots & \ddots \\ & & -1 & 1 \end{bmatrix} \in \mathbb{R}^N.$$

Then the platoon with a disturbance on the leader can be rewritten into

$$\dot{\bar{X}} = [I_N \otimes A - \bar{H} \otimes (BK)]\bar{X} + (e_{N,1} \otimes B)\omega_0$$
 (72)

where $\bar{H} = UHU^{-1}$.

Note that formula (72) and (52) are equivalent, they can be rewritten onto each other with coordinate transformation. With (72), we propose the following proposition.

Proposition 1: For a homogeneous platoon with node model (2) and control law (8). Let μ be defined by (73), and $P_{\bar{H}}$ be a positive definite solution of (74), if there exist two scalars $r_A > 0$ and $\rho > 0$ such that LMI (75) has a positive definite solution to P, then the distributed control gain (76) stabilizes the platoon with a disturbance propagation bound expressed by (77)

$$0 < \mu \le \frac{\lambda_i(\bar{H}) + \lambda_i^*(\bar{H})}{2}, \quad 1 \le i \le q + r$$
 (73)

$$P_{\bar{H}}\bar{H} + \bar{H}^T P_{\bar{H}} - 2\mu P_{\bar{H}} > 0 \tag{74}$$

$$\begin{aligned}
P_{\tilde{H}}\tilde{H} + \tilde{H}^{T}P_{\tilde{H}} - 2\mu P_{\tilde{H}} &> 0 \\
\left[He(AP) + (1 - r_{A})BB^{T} & P \\
P & -1/\rho \right] &< 0
\end{aligned} (74)$$

$$K = \frac{1}{u} r_A B^T P^{-1}$$
 (76)

$$\|C_C \bar{X}/\omega_0\|_{\infty} < \bar{\gamma}_{\rho} = \sqrt{\frac{\lambda_{\max}(P_{\bar{H}})}{\rho \lambda_{\min}(P_{\bar{H}})}}$$
 (77)

where $C_C = I_N \otimes C$, and $C = [1 \ 0 \ 0]$.

The proof of Proposition 1 is similar to that of Theorem 4, which is omitted here for brevity. Note that observe matrix C is added in (77) in order to focus on relative spacing error, i.e., leave out the influence from speed and acceleration. The remarks on Theorem 4 still hold analogously here.

VI. SIMULATION AND DISCUSSION

In this section, numerical examples are provided to validate the effectiveness of the previous theoretical results.

A. Simulation Layout

Consider a platoon with 1 leader and 10 followers, in which each vehicle is represented by a highly nonlinear model. With the inverse model compensation and distributed control law,

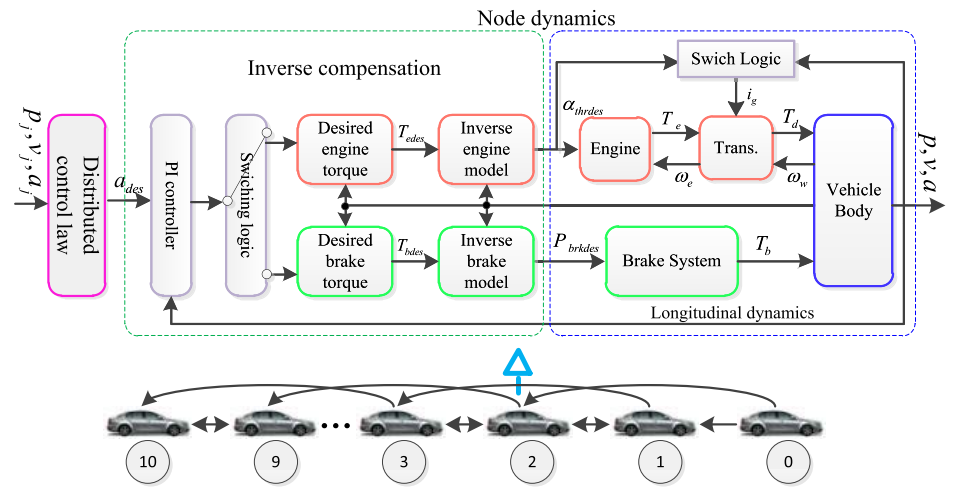


Fig. 4. Layout of a platoon in simulations.

TABLE III

NOMINAL VALUE OF KEY PARAMETERS

Symbol	Unit	Nominal value
M	kg	1600
J_e	$kg \cdot m^2$	0.212
$\eta_{\it T}$		0.92
$ au_e$	S	0.3
i_0		5.83
$egin{array}{c} i_0 \ i_g \end{array}$		[5.56, 2.77, 1.64, 1.00, 0.79]
r_{w}	m	0.30
K_b	N·m/MPa	426
$ au_b$	S	0.3
C_A	kg/m	0.26
f		0.02
g	m/s ²	9.81

the platoon layout can be represented by Fig. 4. The numerical values of the key parameters are listed in Table III.

To yield a proper value of the inertial time delay τ_a , a model identification is applied by using the MATLAB toolbox *ident*, as shown in Fig. 5 [37]. Here, we considered diverse driving conditions, *i.e.*, different operation speed and different wind speed. Seven operation speed points are considered ranging from 20 km/h to 80 km/h, and five wind speed points are taken into account ranging from -54 km/h to 54 km/h. Therefore, totally $7 \times 5 = 35$ identifications were carried out, resulting in the following range of τ_a :

$$0.40 \text{ s} \le \tau_a \le 0.67 \text{ s}. \tag{78}$$

Then, the mean value of (78) is taken for the following simulations, *i.e.*, $\tau_a = 0.54$ s, which is close to the values adopted by [11].

B. Distributed Control Gain

Three communication topologies are considered in the following simulations: TPSF, LPF, and the mixed topology shown in Table II. For brevity, only the procedure of control gain calculation corresponding to TPSF is shown in detail below.

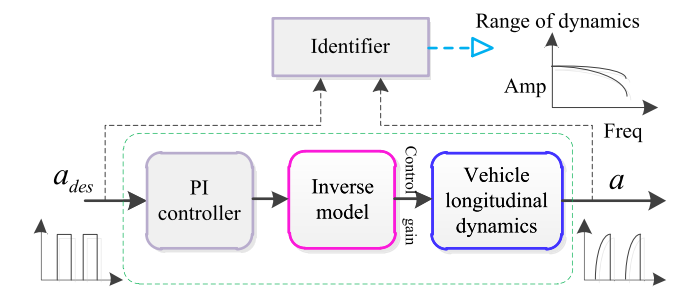


Fig. 5. Procedure of model identification.

The Laplacian matrix and pinning matrix corresponding to TPSF are

$$L_{G} = \begin{bmatrix} 1 & -1 & & & & \\ -1 & 2 & -1 & & & \\ -1 & -1 & 3 & -1 & & \\ & -1 & -1 & 3 & \ddots & \\ & & \ddots & \ddots & \ddots & -1 \\ & & & -1 & -1 & 2 \end{bmatrix} \in \mathbb{R}^{10 \times 10}$$
 (79)

$$P_{G} = \operatorname{diag} \begin{bmatrix} 1 & 1 & 0 & \cdots & 0 & 0 \end{bmatrix} \in \mathbb{R}^{10 \times 10}.$$
 (80)

The eigenvalues of $H = L_G + P_G$ are

$$\lambda_1 = 0.48 \quad \lambda_6 = 3.71$$
 $\lambda_2 = 0.77 \quad \lambda_7 = 4.34 + j0.83$
 $\lambda_3 = 1.29 \quad \lambda_8 = 4.34 - j0.83$
 $\lambda_4 = 2.02 \quad \lambda_9 = 4.09 + j0.42$
 $\lambda_5 = 2.87 \quad \lambda_{10} = 4.09 - j0.42.$ (81)

Thus μ is set as

$$\mu = 0.47.$$
 (82)

Then the Riccati inequality (30) is solved by using the LMI toolbox in MATLAB. The solution of P_0 is

$$P_0 = \begin{bmatrix} 9.55 & -1.22 & -0.17 \\ -1.22 & 1.00 & -0.71 \\ -0.17 & -0.71 & 1.06 \end{bmatrix}.$$
(83)

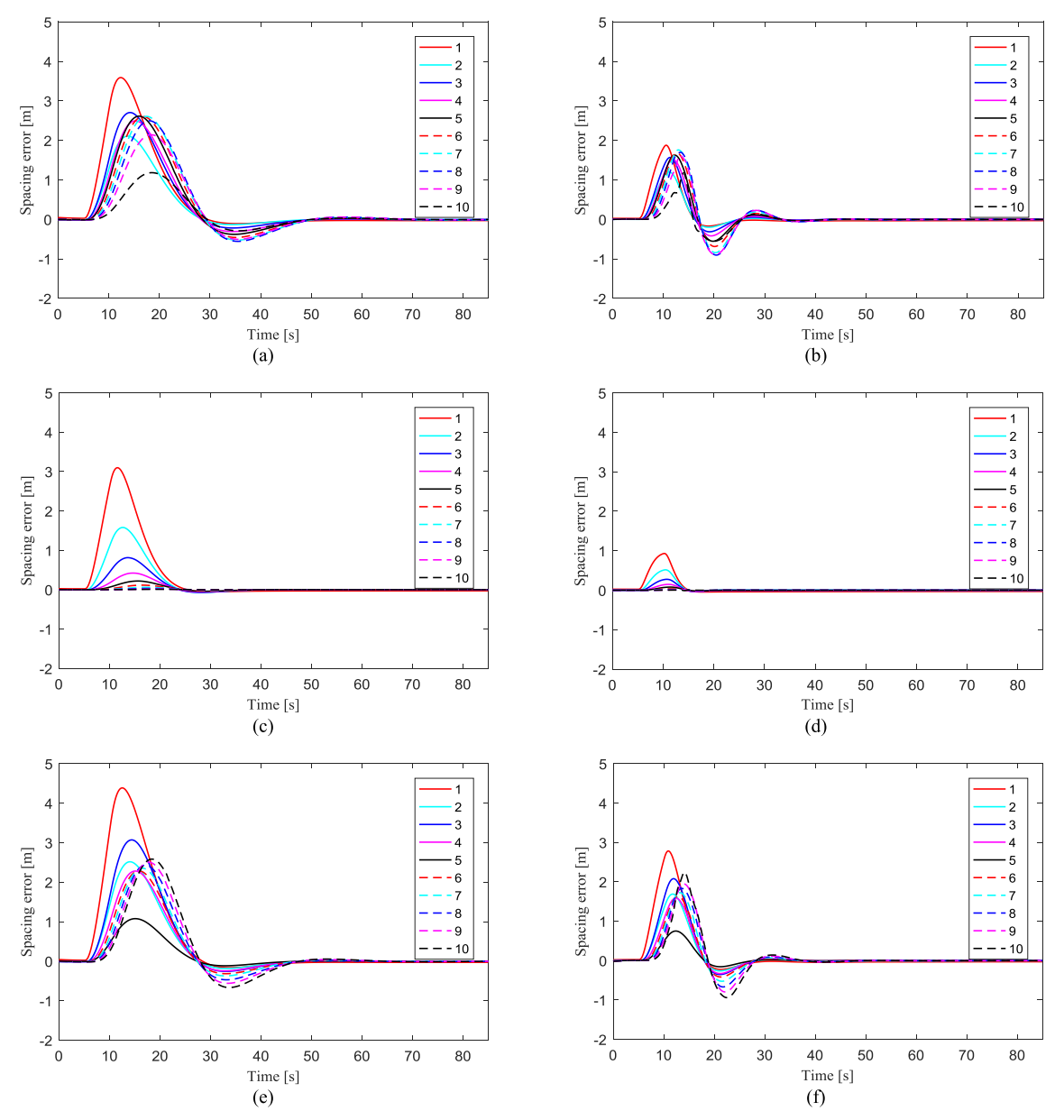


Fig. 6. Simulation results on spacing errors. (a) TPSF—Lower convergence speed. (b) TPSF—Higher convergence speed. (c) LPF—Lower convergence speed. (d) LPF—Higher convergence speed. (e) Mixed—Lower convergence speed. (f) Mixed—Higher convergence speed.

The static feedback gain is calculated through (31)

$$K_{\text{TPSF}} = \frac{B^T P_0^{-1}}{2} = [0.28 \ 1.90 \ 2.19].$$
 (84)

Similarly, we can calculate the feedback gain corresponding to LPF and the mixed topology, *i.e.*,

$$K_{\text{LPF}} = [0.19 \ 1.04 \ 1.11]$$

 $K_{\text{Mixed}} = [0.23 \ 1.51 \ 1.60].$ (85)

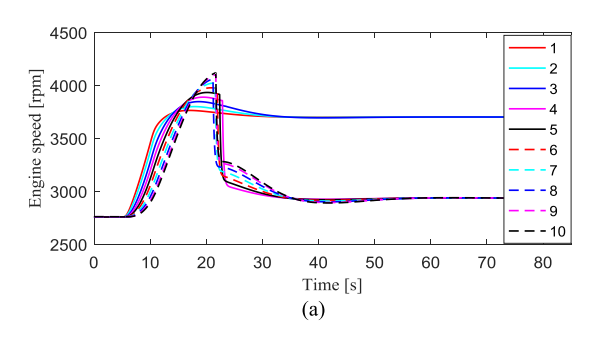
C. Simulation Results

In the simulations, the leader is assumed to follow a desired trajectory as shown

$$v_0 = \begin{cases} 15 \text{ m/s} t \le 5s \\ 15 + 1 \text{ tm/s } 5s < t \le 10 \text{ s} \\ 200 \text{ m/s } 10s < t. \end{cases}$$
 (86)

The initial states of all the followers are set as $x_i(0) = [0 \ 15 \ 0]$, $1 \le i \le 10$. The Simulink toolbox in MATLAB is used to run the nonlinear simulations.

The relative spacing errors of the followers are shown in Fig. 6 on the left side. On the right side of Fig. 6, a comparative result is presented to show the effectiveness of Theorem 3. It is obvious that the algorithm proposed by this paper is valid to provide a feasible control gain that ensures internal stability under various communication topologies. Theorem 3 provides a better convergence speed. The engine speed and throttle angle of the vehicles corresponding to Fig. 6(a) are presented in Fig. 7. Note that the spikes existing in Fig. 7(b) are caused by gear shift. Fig. 8 shows the disturbance propagation performance of topology TPSF, LPF, Mixed, and PF. Input disturbance is designed as $\omega_0 = 0.75 \sin(\pi t/10)$. As shown in Fig. 8, relative spacing errors of the TPSF and LPF are bounded, which is actually



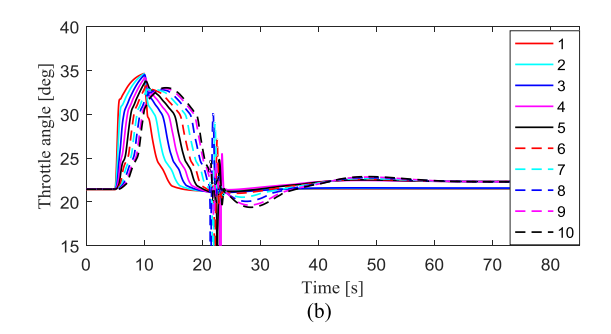
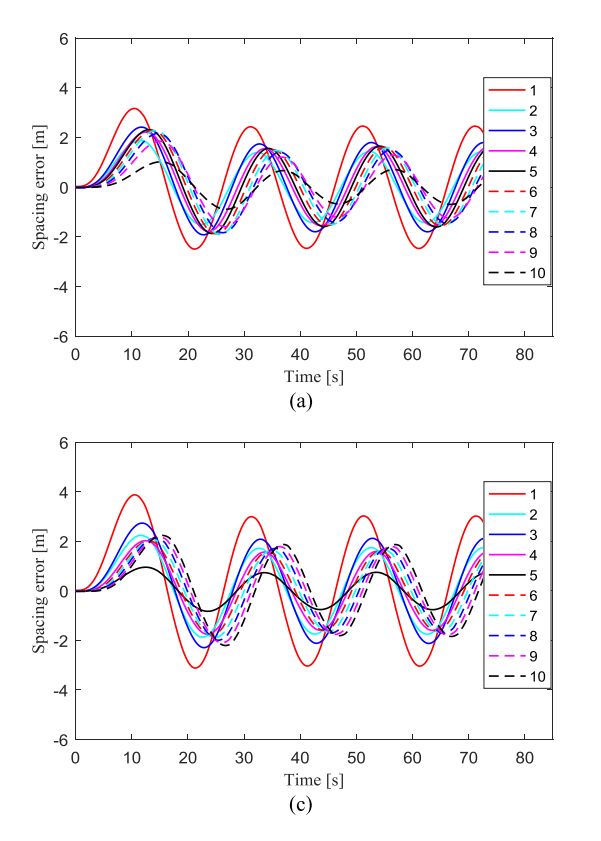


Fig. 7. Simulation results on vehicle status. (a) Engine speed. (b) Throttle angle.



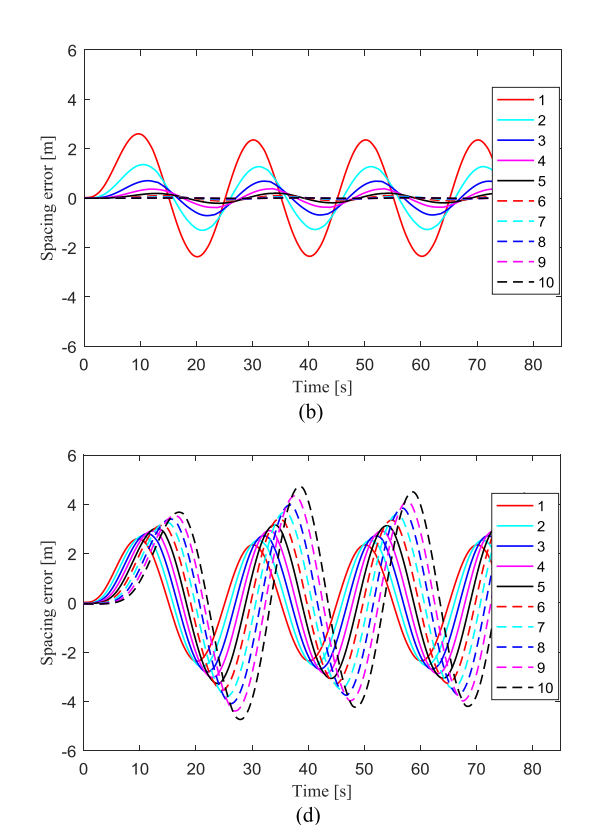


Fig. 8. Results of disturbance propagation. (a) TPSF. (b) LPF. (c) Mix. (d) PF.

their intrinsic property. The performance of the mixed topology is determined by its subcomponents, *i.e.*, TPSF and PF. The TPSF subpart will attenuate relative spacing error, while the PF subpart will amplify relative spacing error under certain input frequencies. To better support the statement, Fig. 8(d) is given. It is obvious that disturbance amplifies along the platoon with PF topology.

Note that disturbance propagation is mainly determined by the topology, while control gain only has limited influence. The statement is supported by Fig. 9, in which we investigated the relationship among disturbance propagation upper bound, topology, control gain and platoon size. By writing disturbance propagation upper bound, we mean $\bar{\gamma}_{\rho}$ defined in (77). In Fig. 9(a), a platoon with topology BPF and the two control gains in Table IV is studied. Note that K_1 and K_2 share the same $\bar{\gamma}_{\rho}$, because the same ρ is used in their calculation (by using Proposition 1). The red line in Fig. 9(a)

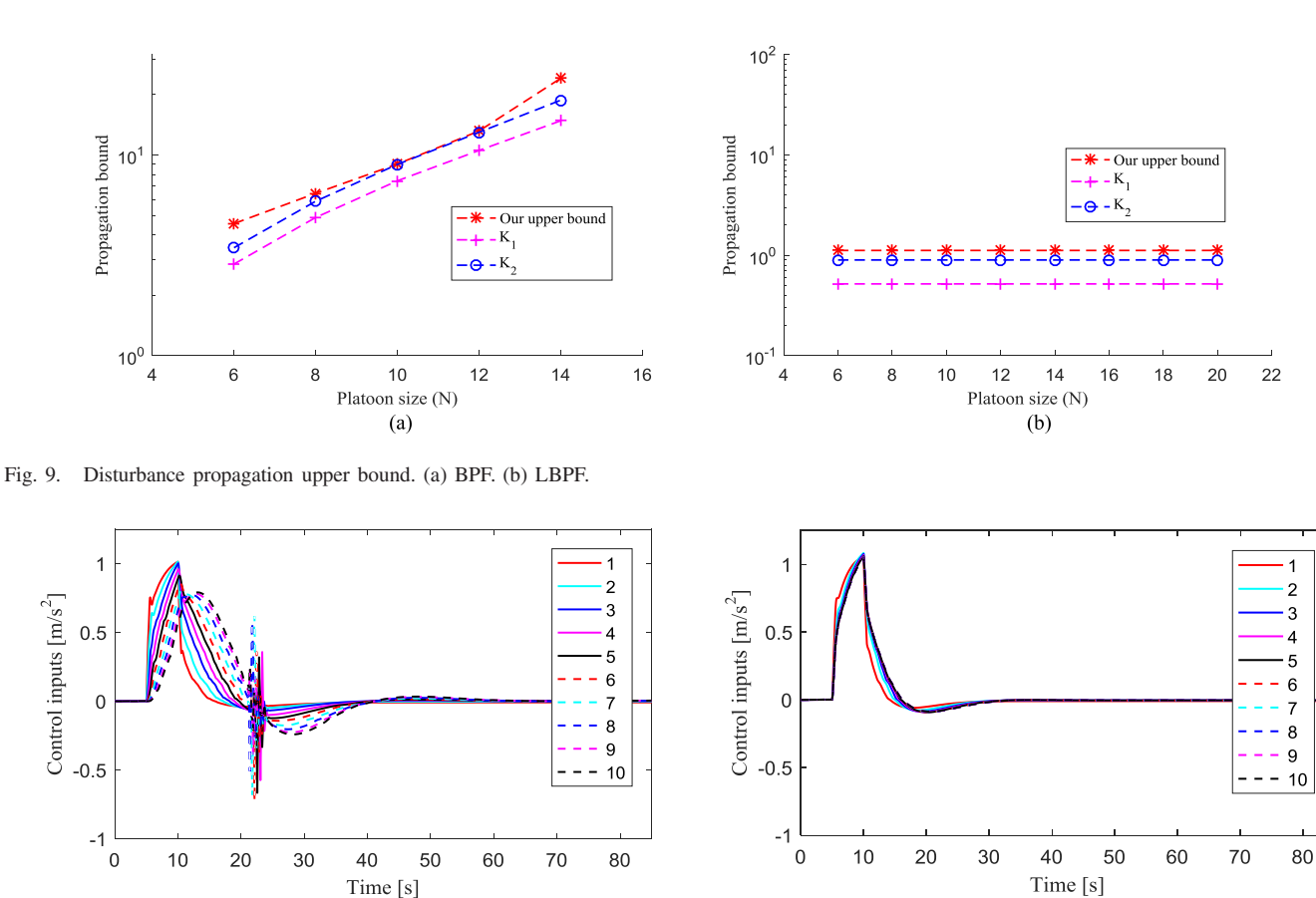
TABLE IV
STABILIZING CONTROL GAIN

Topology	BPF	LBPF
K_1	[6.0 30. 16.1]	[1.9 4.9 2.3]
K_2	[5.0 25.1 13.3]	[1.12 3.0 1.4]

specifies the bound provided by Proposition 1, *i.e.*, $\bar{\gamma}_{\rho}$. Since the maximum platoon size involved here is 20, which is not very large, the norm of the platoon transfer function can be numerically calculated by MATLAB, *i.e.*, $\|C_C\bar{X}/\omega_0\|_{\infty}$. And the numerically calculated norm can be viewed as the true performance of the platoon. In Fig. 9(a), the magenta and blue lines represent the true performance corresponding to K_1 and K_2 , respectively. Same goes for Fig. 9(b).

13

Control inputs [m/s²]



(a) (b) Control inputs [m/s²] Control inputs [m/s²] 3 3 4 5 8 9 9 -0.5 10 -1 0 50 10 20 30 40 60 70 80 0 10 20 30 40 50 60 70 80 Time [s] Time [s]

Fig. 10. Control inputs (i.e., desired acceleration). (a) TPSF. (b) LPF. (c) Mix. (d) PF.

From Fig. 9, we can see that different topologies have different performances on disturbance propagation. The $\bar{\gamma}_{\rho}$ of LBPF does not amplify along with platoon size, while the $\bar{\gamma}_{\rho}$ of BPF goes up. Different control gains can change the propagation performance, i.e., $\|C_C X/\omega_0\|_{\infty}$. But this change does not alter the trend of the norm along with the platoon size. For BPF with K_1 , the norm goes up along with the platoon size, with the other control gain K_2 , the norm still goes up. It can also be seen from Fig. 9 that the $\bar{\gamma}_{\rho}$ proposed by Proposition 1 has the same trend to the numerically calculated norm $\|C_C \bar{X}/\omega_0\|_{\infty}$. The $\bar{\gamma}_{\rho}$ proposed by Proposition 1 is valid for not only one control gain, but also a set of control gains. For some of them, $\bar{\gamma}_{\rho}$ is very close to $left \|C_C \bar{X}/\omega_0\|_{\infty}$. Yet for other control gains, $\bar{\gamma}_{\rho}$ may be a bit farther from $\|C_C X/\omega_0\|_{\infty}$.

To see if the control inputs (desired accelerations) provided by controller K are compatible with driving comfort, we plotted the control inputs (see Fig. 10) corresponding to the simulation shown in Fig. 6 (left column). It can be seen from Fig. 10 as follows.

- 1) Different topologies can lead to different control inputs, which means that distributed controller is topologically
- 2) The control inputs are compatible with driving comfort since the desired values are in the range of [-2.5, 1.5]m/s², which is often used in the design

of ACC systems. Increasing the control gain *K* or the magnitude of the leader behavior will both increase the control inputs (i.e., desired acceleration).

VII. CONCLUSION

This paper studied the internal stability and controller synthesis for vehicular platoons with generic communication topologies. For theoretical analysis, a linear vehicle model was derived by using the inverse model compensation. Directed graph was employed to model the communication topologies, resulting in a linear time invariant closed-loop platoon model when employing the constant spacing policy.

The main conclusions are summarized as follows. Theorem 1 provides a sufficient and necessary condition for platoons to achieve internal stability. Theorems 2 and 3 present two Riccati inequality based algorithms to compute the feedback gains. The overall upper bound of the spacing errors due to disturbance on the input of the leader is explicitly provided, showing that the structure of the topology mainly determines the disturbance propagation performance.

One future work is to address internal stability with generic communication topology subjected to communication failure and delay. Also, since vehicles in real traffic are heterogeneous, stability of heterogeneous platoon is another important problem that is worth further investigation.

REFERENCES

- [1] J. Capp and B. Litkouhi, "The rise of the crash-proof car," *IEEE Spectr.*, vol. 51, no. 5, pp. 32–37, May 2014.
- [2] S. E. Li, K. Deng, Y. Zheng, and H. Peng, "Effect of pulse-and-glide strategy on traffic flow for a platoon of mixed automated and manually driven vehicles," *Comput.-Aided Civil Infrast. Eng.*, vol. 30, no. 11, pp. 892–905, 2015.
- [3] S. E. Li et al., "Kalman filter-based tracking of moving objects using linear ultrasonic sensor array for road vehicles," Mech. Syst. Signal Process., vol. 98, pp. 173–189, Jan. 2018.
- [4] J.-Q. Wang, S. E. Li, Y. Zheng, and X.-Y. Lu, "Longitudinal collision mitigation via coordinated braking of multiple vehicles using model predictive control," *Integr. Comput.-Aided Eng.*, vol. 22, no. 2, pp. 171–185, 2015.
- [5] S. Öncü, J. Ploeg, N. van de Wouw, and H. Nijmeijer, "Cooperative adaptive cruise control: Network-aware analysis of string stability," *IEEE Trans. Intell. Transp. Syst.*, vol. 13, no. 4, pp. 1527–1537, Aug. 2014.
- [6] Y. Zheng, S. Li, K. Li, and L.-Y. Wang, "Stability margin improvement of vehicular platoon considering undirected topology and asymmetric control," *IEEE Trans. Control Syst. Technol.*, vol. 24, no. 4, pp. 1253–1265, Jul. 2016.
- [7] R. Rajamani, H.-S. Tan, B. K. Law, and W.-B. Zhang, "Demonstration of integrated longitudinal and lateral control for the operation of automated vehicles in platoons," *IEEE Trans. Control Syst. Technol.*, vol. 8, no. 4, pp. 695–708, Jul. 2000.
- [8] S. E. Li, R. Li, J. Wang, X. Hu, B. Cheng, and K. Li, "Stabilizing periodic control of automated vehicle platoon with minimized fuel consumption," *IEEE Trans. Transport. Electrific.*, vol. 3, no. 1, pp. 259–271, Mar. 2017.
- [9] E. V. Nunen, M. R. J. A. E. Kwakkernaat, J. Ploeg, and B. D. Netten, "Cooperative competition for future mobility," *IEEE Trans. Intell. Transp. Syst.*, vol. 13, no. 3, pp. 1018–1025, Sep. 2012.
- [10] S. E. Li et al., "Dynamical modeling and distributed control of connected and automated vehicles: Challenges and opportunities," *IEEE Intell. Transp. Syst. Mag.*, vol. 9, no. 3, pp. 46–58, Jul. 2017.
- [11] Y. Zheng, S. E. Li, J. Wang, D. Cao, and K. Li, "Stability and scalability of homogeneous vehicular platoon: Study on the influence of information flow topologies," *IEEE Trans. Intell. Transp. Syst.*, vol. 17, no. 1, pp. 14–26, Jan. 2016.
- [12] H. Hao and P. Barooah, "Stability and robustness of large platoons of vehicles with double-integrator models and nearest neighbor interaction," *Int. J. Robust Nonlinear Control*, vol. 23, no. 18, pp. 2097–2122, 2013.

- [13] A. Ghasemi, R. Kazemi, and S. Azadi, "Stable decentralized control of a platoon of vehicles with heterogeneous information feedback," *IEEE Trans. Veh. Technol.*, vol. 62, no. 9, pp. 4299–4308, Nov. 2013.
- [14] J. Ploeg, D. P. Shukla, N. van de Wouw, and H. Nijmeijer, "Controller synthesis for string stability of vehicle platoons," *IEEE Trans. Intell. Transp. Syst.*, vol. 15, no. 2, pp. 854–865, Apr. 2014.
- [15] S. E. Li, Q. Guo, L. Xin, B. Cheng, and K. Li, "Fuel-saving servoloop control for an adaptive cruise control system of road vehicles with step-gear transmission," *IEEE Trans. Veh. Technol.*, vol. 66, no. 3, pp. 2033–2043, Mar. 2017.
- [16] S. E. Li, Y. Zheng, K. Li, and J. Wang, "An Overview of vehicular platoon control under the four-component framework," in *Proc. IEEE Intell. Vehicle Symp.*, Seoul, South Korea, Jun. 2015, pp. 286–291.
- [17] S. S. Stankovic, M. J. Stanojevic, and D. D. Siljak, "Decentralized overlapping control of a platoon of vehicles," *IEEE Trans. Control Syst. Technol.*, vol. 8, no. 5, pp. 816–832, Sep. 2000.
- [18] C.-Y. Liang and H. Peng, "String stability analysis of adaptive cruise controlled vehicles," JSME Int. J. C Mech. Syst., Mach. Elements Manuf., vol. 43, no. 3, pp. 671–677, 2000.
- [19] Y. Zhang, E. B. Kosmatopoulos, P. A. Ioannou, and C. C. Chien, "Using front and back information for tight vehicle following maneuvers," *IEEE Trans. Veh. Technol.*, vol. 48, no. 1, pp. 319–328, Jan. 1999.
- [20] P. Seiler, A. Pant, and K. Hedrick, "Disturbance propagation in vehicle strings," *IEEE Trans. Autom. Control*, vol. 49, no. 10, pp. 1835–1841, Oct. 2004.
- [21] R. H. Middleton and J. H. Braslavsky, "String instability in classes of linear time invariant formation control with limited communication range," *IEEE Trans. Autom. Control*, vol. 55, no. 7, pp. 1519–1530, Jul. 2010.
- [22] J. Zhou and H. Peng, "Range policy of adaptive cruise control vehicles for improved flow stability and string stability," *IEEE Trans. Intell. Transp. Syst.*, vol. 6, no. 2, pp. 229–237, Jun. 2005.
- [23] Y. Yao, L. Rao, and X. Liu, "Performance and reliability analysis of IEEE 802.11p safety communication in a highway environment," *IEEE Trans. Veh. Technol.*, vol. 62, no. 9, pp. 4198–4212, Nov. 2013.
- [24] Y. S. Krishna, S. Darbha, and K. R. Rajagopal, "Information flow and its relation to the stability of the motion of vehicles in a rigid formation," in *Proc. Amer. Control Conf.*, Jun. 2005, pp. 1853–1858.
- [25] Y. Zheng, S. E. Li, K. Li, F. Borrelli, and J. K. Hedrick, "Distributed model predictive control for heterogeneous vehicle platoons under unidirectional topologies," *IEEE Trans. Control Syst. Technol.*, vol. 25, no. 3, pp. 899–910, Mar. 2017.
- [26] S. Li, K. Li, R. Rajamani, and J. Wang, "Model predictive multiobjective vehicular adaptive cruise control," *IEEE Trans. Control Syst. Technol.*, vol. 19, no. 3, pp. 556–566, May 2011.
- [27] J. A. Fax and R. M. Murray, "Information flow and cooperative control of vehicle formations," *IEEE Trans. Autom. Control*, vol. 49, no. 9, pp. 1465–1476, Sep. 2004.
- [28] G. Guo and W. Yue, "Sampled-data cooperative adaptive cruise control of vehicles with sensor failures," *IEEE Trans. Intell. Transp. Syst.*, vol. 15, no. 6, pp. 2401–2418, Dec. 2014.
- [29] F. Lin, M. Fardad, and M. R. Jovanovic, "Optimal control of vehicular formations with nearest neighbor interactions," *IEEE Trans. Autom. Control*, vol. 57, no. 9, pp. 2203–2218, Sep. 2012.
- [30] S. E. Li, F. Gao, D. Cao, and K. Li, "Multiple-model switching control of vehicle longitudinal dynamics for platoon-level automation," *IEEE Trans. Veh. Technol.*, vol. 65, no. 6, pp. 4480–4492, Jun. 2016.
- [31] F. Gao, S. E. Li, Y. Zheng, and D. Kum, "Robust control of heterogeneous vehicular platoon with uncertain dynamics and communication delay," *IET Intell. Transp. Syst.*, vol. 10, no. 7, pp. 503–513, 2016.
- [32] A. Jadbabaie, J. Lin, and A. S. Morse, "Coordination of groups of mobile autonomous agents using nearest neighbor rules," *IEEE Trans. Autom. Control*, vol. 48, no. 6, pp. 988–1001, Jun. 2003.
- [33] R. Olfati-Saber and R. M. Murray, "Consensus problems in networks of agents with switching topology and time-delays," *IEEE Trans. Autom. Control*, vol. 49, no. 9, pp. 1520–1533, Sep. 2004.
- [34] W. Ren and R. W. Beard, "Consensus seeking in multiagent systems under dynamically changing interaction topologies," *IEEE Trans. Autom. Control*, vol. 50, no. 5, pp. 655–661, May 2005.
- [35] R. Horn and C. Johnson, *Matrix Analysis*. Cambridge, U.K.: Cambridge Univ. Press, sec. 3.4, 2012, pp. 201–213.
- [36] P. P. Khargonekar, I. R. Petersen, and K. Zhou, "Robust stabilization of uncertain linear systems: Quadratic stabilizability and H_{∞} control theory," *IEEE Trans. Autom. Control*, vol. 35, no. 3, pp. 356–361, Mar. 1990.

- [37] S. E. Li, X. Qin, K. Li, J. Wang, and B. Xie, "Robustness analysis and controller synthesis of homogeneous vehicular platoons with bounded parameter uncertainty," *IEEE/ASME Trans. Mechatronics*, vol. 22, no. 2, pp. 1014–1025, Apr. 2017.
- [38] E. Shaw and J. Hedrick, "String stability analysis for heterogeneous vehicle strings," in *Proc. Amer. Control Conf.*, Jul. 2007, pp. 3118–3125.
- [39] I. Saboori and K. Khorasani, "H_∞ consensus achievement of multiagent systems with directed and switching topology networks," *IEEE Trans. Autom. Control*, vol. 59, no. 11, pp. 3104–3109, Nov. 2014.
- [40] L. Xiao and F. Gao, "Practical string stability of platoon of adaptive cruise control vehicles," *IEEE Trans. Intell. Transp. Syst.*, vol. 12, no. 4, pp. 1184–1194, Dec. 2011.
- [41] M. di Bernardo, A. Salvi, and S. Santini, "Distributed consensus strategy for platooning of vehicles in the presence of time-varying heterogeneous communication delays," *IEEE Trans. Intell. Transp. Syst.*, vol. 16, no. 1, pp. 102–112, Feb. 2015.

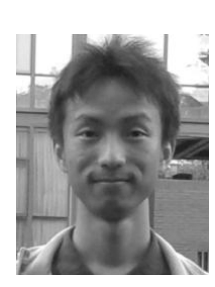


Shengbo Eben Li (M'12–SM'16) received the M.S. and Ph.D. degrees from Tsinghua University Beijing, China, in 2006 and 2009, respectively.

He was with Stanford University, Stanford, CA, USA; the University of Michigan, Ann Arbor, MI, USA; and the University of California Berkeley, Berkeley, CA, USA. He is currently an Associate Professor with the Department of Automotive Engineering, Tsinghua University. He has authored or coauthored over 100 peer-reviewed journal/conference papers, and the co-inventor of over 20 Chinese

patents. His current research interests include intelligent and connected vehicles, learning-based driver assistance, distributed control and optimal estimation, and electrified powertrain management.

Dr. Li was a recipient of the Best Paper Award in 2014 IEEE Intelligent Transportation System Symposium, the Best Paper Award in 14th ITS Asia Pacific Forum, National Award for Technological Invention in China in 2013, the Excellent Young Scholar of NSF China in 2016, and the Young Professorship of Changjiang Scholar Program in 2016. He is the TPC Member of IEEE Intelligent Vehicle Symposium and the ISC Member of FAST-zero 2017 in Japan. He is an Associate editor of the IEEE Intelligent Transportation Systems Magazine and IEEE TRANSACTIONS ON INTELLIGENT TRANSPORTATION SYSTEMS.



Xiaohui Qin received the B.E. degree from Tsinghua University, Beijing, China, in 2010, where he is currently pursuing the Ph.D. degree in advance in automotive engineering with the College of Mechanical Engineering.

His current research interest includes cooperative platooning control.



Yang Zheng received the B.E. and M.E. degrees from Tsinghua University, Beijing, China, in 2013 and 2015, respectively. He is currently pursuing the D.Phil. (Ph.D.) degree with the Department of Engineering Science, University of Oxford, Oxford, U.K.

His current research interests include distributed control of dynamical system over networks with applications on vehicular platoon.

Mr. Zheng was a recipient of the Best Student Paper Award at the 17th International IEEE Confer-

ence on Intelligent Transportation Systems in 2014, and the Best Paper Award at the in 14th Intelligent Transportation Systems Asia-Pacific Forum in 2015. He was a recipient of the National Scholarship and Outstanding Graduate in Tsinghua University.



Jianqiang Wang received the B.Tech., M.S., and Ph.D. degrees from Jilin University, Changchun, China, in 1994, 1997, and 2002, respectively.

He is currently an Associate Professor with the Department of Automotive Engineering, State Key Laboratory of Automotive Safety and Energy, Tsinghua University, Beijing, China. He has authored or co-authored over 40 journal papers, and he is the co-holder of 30 patent applications. His current research interests include intelligent vehicles, driving assistance systems, and driver behavior.

Dr. Wang has involved in over ten sponsored projects, and he was a recipient of nine awards.



Keqiang Li received the B.Tech. degree from Tsinghua University, Beijing, China, in 1985, and the M.S. and Ph.D. degrees from Chongqing University, Chongqing, China, in 1988 and 1995, respectively.

He is a Professor of automotive engineering with Tsinghua University. He has authored or co-authored over 90 papers and is a co-inventor of 12 patents in China and Japan. His current research interests include vehicle dynamics and control for driver assistance systems and hybrid electrical vehicle.

Dr. Li was a Senior Member of the Society of Automotive Engineers of China, and on the editorial boards of the *International Journal of Intelligent Transportation Systems Research* and the *International Journal of Vehicle Autonomous Systems*. He was a recipient of the "Changjiang Scholar Program Professor" and some awards from public agencies and academic institutions of China.



Hongwei Zhang (S'01–M'07–SM'13) received the B.S. and M.S. degrees in computer engineering from Chongqing University, Chongqing, China, and the Ph.D. degree in computer science and engineering from The Ohio State University, Columbus, OH, USA.

He is currently an Associate Professor of electrical and computer engineering with Iowa State University, Ames, IA, USA. His research has been an integral part of several NSF and DARPA programs such as the NSF CPS, NSF GENI, and DARPA

NEST program. His current research interests include modeling, algorithmic, and systems issues in wireless sensing and control networks as well as their applications in connected and automated vehicles, smart energy grid, industrial automation, and cyber-physical systems in general.

Dr. Zhang was a recipient of the NSF CAREER Award.